CRYSTAL GROWTH & DESIGN

Article

Synthesis and characterization of a series of sulfamethazine multi-component crystals with various benzoic acids

Matthew Clarke Scheepers, and Andreas Lemmerer

Cryst. Growth Des., **Just Accepted Manuscript** • DOI: 10.1021/acs.cgd.9b01209 • Publication Date (Web): 18 Dec 2019

Just Accepted

is published by the American Chemical Society. 1155 Sixteenth Street N.W., Washington, DC 20036

Synthesis and characterization of a series of sulfamethazine multi-component crystals with various benzoic acids

Matthew C. Scheepers and Andreas Lemmerer*‡

‡*Molecular Sciences Institute, School of Chemistry, University of the Witwatersrand, 2050, Johannesburg, South Africa*

RECEIVED DATE (to be automatically inserted after your manuscript is accepted if required according to the journal that you are submitting your paper to)

To whom correspondence should be addressed:

Dr. Andreas Lemmerer, Molecular Sciences Institute, School of Chemistry, University of the Witwatersrand, Private Bag 3, 2050, Johannesburg, South Africa.

E-mail: andreas.lemmerer@wits.ac.za. Fax: +27-11-717-6749. Tel: +27-11-717-6711.

ABSTRACT:

Nine multi-component crystals consisting of sulfamethazine (sz) with benzoic acid and its derivatives were synthesized and characterized. Eight of the nine multi-component crystals are co-crystals, while one is a molecular salt. The co-formers used to form multi-component crystals with sz include: 2-chloro-4-nitrobenzoic acid (2c4n), 2-chloro-5-nitrobenzoic acid (2c5n), salicylic acid (2hba), 3-hydroxybenzoic acid (3hba), 4-hydroxybenzoic acid (4hba), 4-bromobenzoic acid (4Brba), benzoic acid (ba), cinnamic acid (ca) and toluic acid (ta). These multi-component crystals were characterized by single-crystal X-ray diffraction (SC-XRD), Powder X-ray diffraction (PXRD) and Differential Scanning Calorimetry (DSC). SC-XRD showed that eight of the co-formers that interacted with sz formed the amidine-carboxyl synthon; with the only exception to this were **sz+4hba** which formed the imidine-carboxyl synthon formed instead. PXRD confirmed that the single crystals were representative of the bulk material. DSC showed most of the multi-component crystals to have only a melting phase transition, which differed from the melting points of the co-formers. The only exceptions were **sz+4brba** and **sz+ca**, where an additional endothermic peak was observed, which corresponds to an amorphous phase transition before melting.

KEYWORDS:

sulfamethazine, sulfadiazine, co-crystal, salt, multi-component crystal

Introduction

The need for designing new crystal forms of potentially useful Active Pharmaceutical Ingredients (API's) has been rising in the past few decades. Promising drug candidates often have poor physiochemical properties, especially poor water solubility and dissolution rates [1] [2]. One common approach to altering the poor physiochemical properties of an API is to incorporate them into multi-component crystals[3]. Multi-component crystals often have different properties, if not superior properties, in respect to its co-formers[4]. Therefore there is a great interest in exploring new multi-component crystals of various APIs.

Sulfamethazine (sz), also referred to as sulfadimidine, is an anti-bacterial drug used to treat urinary tract infection, chlamydia, malaria, rheumatoid fever and toxoplasmosis in humans as well as for veterinary

purposes. [5] Sz is also known to be tautomeric, [5, 6] consisting of an amidine form and an imidine form (**Scheme 1**). Both forms have been reported to appear in the solid state. [5, 6, 7] However, the amidine form tends to be the more dominant form, appearing more frequently than the imidine form. In its pure form sz is able to crystallise into several different crystal habits, but has only one crystal structure. [8] In addition to the amidine/imidine group, an amino group is present to act as an additional hydrogen bond donor, and the sulfoxide and second nitrogen of the pyrimidine ring can act as an additional hydrogen bond acceptor. This provides a wide variety of possible hydrogen bond interactions to occur.

Several different co-crystals and solvates of sulfamethazine have already been reported in the literature. The major synthon that forms between sz and the corresponding co-formers involves the amidine/imidine functional group. Several multi-component crystals of sz containing a co-former with a carboxylic acid usually interact with the amidine/imidine group as seen in synthon (i) and (ii) (**Scheme 2**). In such case, this should leave the amino and sulfoxide groups free to interact with each other (Synthon (iii), **Scheme 2**).

In this work we present the synthesis of 9 multi-component crystals of sulfamethazine, with eight co-crystals and one molecular salt. Six of these multi-component crystals are novel while three have been previously reported but produced under slightly different conditions. The benzoic acids chosen for this work were either structural isomers of each other (**2hba, 3hba, 4hba etc.**) or did not contain any additional hydrogen bonding groups (e.g. **ca, ba, ta**). These multi-component crystals were characterized by Single Crystal X-ray Diffraction (SC-XRD), Powder X-ray diffraction (PXRD) and Differential Scanning Calorimetry (DSC).

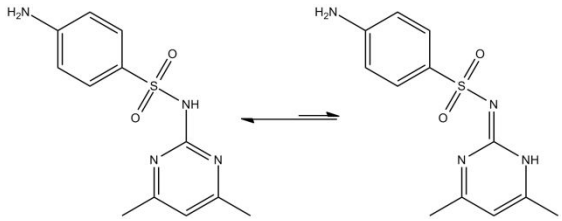

Scheme 1. Sulfamethazine showing the amidine form (left) and imidine form (right).

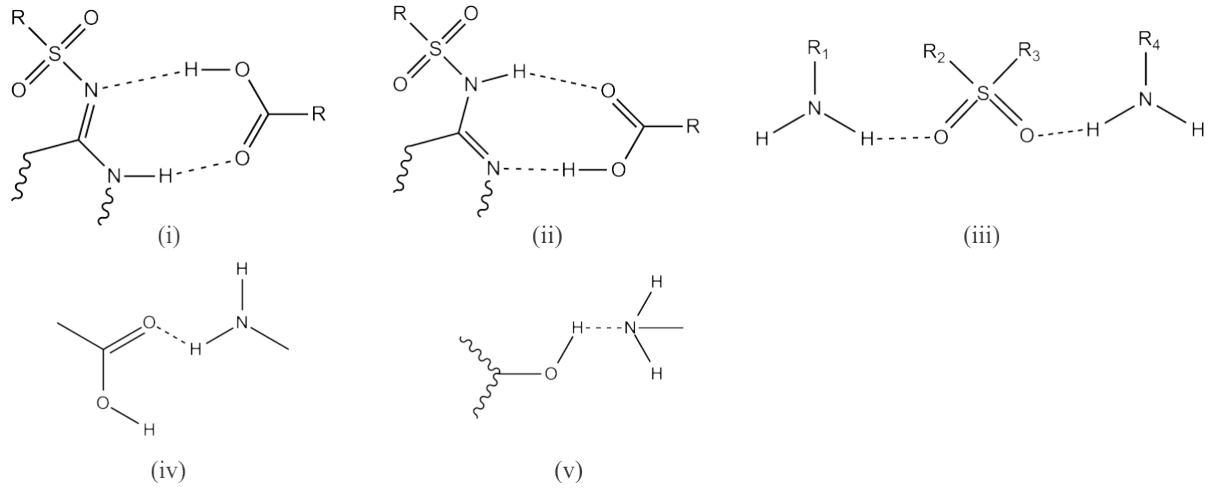

Scheme 2 Some of the synthons expected for this work: (i) amidine-carboxyl synthon, (ii) imidine-carboxyl synthon, (iii) sulfoxide-amino chains, (iv) amino-carboxyl synthon, (v) Hydroxyl-amino synthon.

Experimental Section

Crystal Preparation

All reagents used were purchased from Sigma-Aldrich and were used without further purification.

Most of the co-crystals presented here have been prepared almost exclusively by solvent evaporation methods. Equimolar amounts of SZ and the respective co-former were dissolved together in a 1:1 v/v ratio of ethanol: acetonitrile, which was allowed to stir for an additional 10 minutes with some heating. Afterwards samples were left slightly open at room temperature to allow solvent evaporation. Crystals were grown from this solution after several days.

For the case of **sz+2c5n** and **sz+ca**, ball milling followed by solvent evaporation methods was deployed. Equimolar amounts of sz and the respective co-former were placed in Teflon-coated milling jar (18mm diameter, 65 mm length) with two steel balls (5mm diameter). A few drops of acetonitrile were added to this mixture. The jars were then placed on a Retsch MM200 vibratory mill and were milled at 20 Hz for 20 minutes. Afterwards the solvent evaporation methods described previously was used, with some of the powder from the ball milling used as seeds.

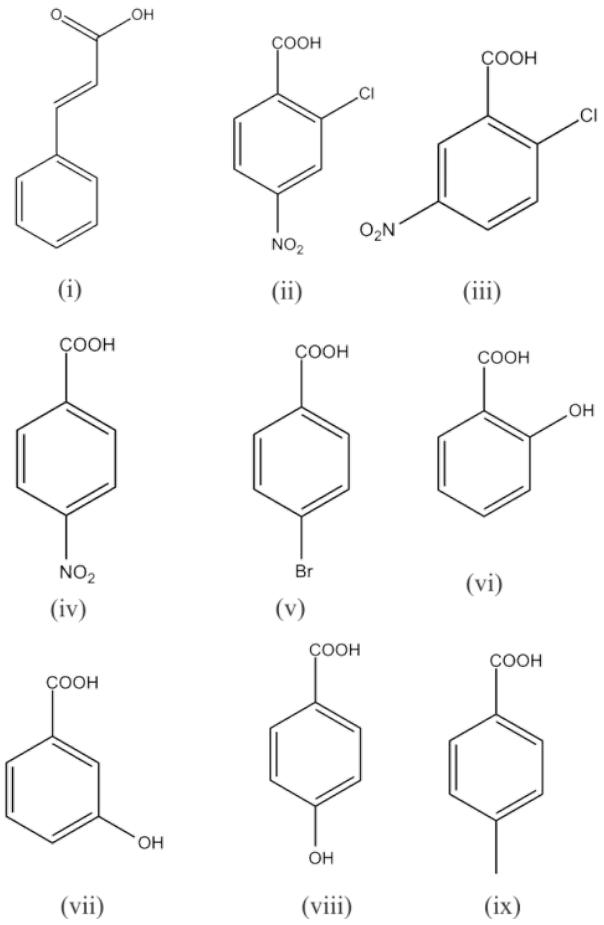

Scheme 3: Co-formers used for this work: (i) cinnamic acid (ca), (ii) 2-chloro-4-nitrobenzoic acid (2c4n), (iii) 2-chloro-5-nitrobenzoic acid (2c5n), (iv) 4-nitrobenzoic acid (4nba), (v) 4-bromobenzoic acid (4brba), (vi) 2-hydroxybenzoic acid/salicylic acid (2hba), (vii) 3-hydroxybenzoic acid (3hba), (viii) 4-hydroxybenzoic acid (4hba), (ix) toluic acid (ta).

Powder X-ray Diffraction (PXRD)

Powder X-ray diffraction is done to determine the phase purity of the bulk material. PXRD data for all compounds were measured at 293 K on a Bruker D2 Phaser diffractometer which employs a sealed tube Co X-ray source (λ = 1.78896 Å), operating at 30 kV and 10 mA, and LynxEye PSD detector in Bragg-Brentano geometry. Powder patterns for each sample are presented in the supporting information, where the experimentally obtained data are compared to the calculated patterns obtained from the SC-XRD data.

Single Crystal X-Ray Diffraction (SC-XRD)

The Bruker D8 VENTURE PHOTON CMOS area detector diffractometer, equipped with a graphite monochromated Mo $K\alpha_1$ sealed tube (50 kV, 30 mA), was used to collect all the intensity data. The program *SAINT+*, vers. 6.02 [9] was used to integrate the data and the program *SADABS* [10] was used to make empirical absorption corrections. Space group assignments were made using *XPREP* [10] on all compounds. In all cases, the structures were solved in the *WinGX* Suite of programs [11] by direct methods using *SHELXS-97* [10] and refined using full-matrix least-squares/difference Fourier techniques on F^2 using *SHELXL-97*. [10] All non-hydrogen atoms were refined anisotropically. Thereafter, all hydrogen atoms attached to N or O atoms, except where otherwise stated, were located in the difference Fourier map and their coordinates and isotropic thermal displacement parameters were refined freely. All C-H hydrogen atoms were placed at idealized positions and refined as riding atoms with isotropic parameters 1.2 or 1.5 times those of the 'heavy' atoms to which they are attached. Diagrams and publication material were generated using *ORTEP-3*, [11] and *Mercury* [12].

Differential Scanning Calorimetry (DSC)

Differential scanning calorimetry data were collected using a Mettler Toledo 822^e with aluminium pans under nitrogen gas (flow rate = 10 L/min). Exothermic events were shown as peaks. Co-crystals were heated and cooled to determine melting points as well as any additional phase transitions. The temperature and energy calibrations were performed using pure indium (purity 99.99%, m.p 156.6°C, heat of fusion: 28.45 J g^{-1}).

Infrared Spectroscopy

Infrared spectra were collected on a Bruker Tensor 27. Samples were used as is without further processing. Spectra were collected in the range of 4000-600 cm^{-1} and band intensities were expressed as transmittance %.

Results and Discussion

Nine multi-component crystal forms containing sulfamethazine are reported. Six of these crystal forms are new. These crystal forms were characterized by SC-XRD. PXRD was used to confirm that the bulk material matched the calculated pattern in order to ensure purity. DSC was used to determine the melting points as well as any other potential phase transitions.

SC-XRD Results

Sz formed nine multi-component crystals which were characterized by SC-XRD. For most of these crystal systems the intermolecular interactions are similar, and possess some structural and packing similarities. For the purpose of this work, several multi-component crystals are grouped and discussed together below. **Table 1** gives a list of which multi-component crystals are grouped together and reasons for such grouping. In addition, **Table 4** contains a list of the bond lengths of the carboxyl group obtained from each of the multi-component crystals as well as if a salt or co-crystal was formed. The ratios of the C-O bond lengths indicate that most of the crystals systems are co-crystals, with the exception of **sz**+**2c4n** and **sz**+**3hba** which show incomplete proton transfer.

Table 1 The grouping of the multi-component crystals as well as the motivation for such groupings.

Group	Motivation for grouping together
sz + 4Brba	**sz + 4Brba** is in its own group since it does not fit in with the other three group list below.
sz + ca, **sz + ba**, **sz + ta**	The co-formers consist of a carboxylic acid group which acts as the sole source for hydrogen bonding.
sz + 2hba, **sz + 3hba**, **sz + 4hba**	The co-formers are structural isomers of each other.
sz + 2c4n, **sz + 2c5n**	The co-formers are structural isomers of each other, in particular it is the shift of the nitro group from the 4' position to the 5' position.

Table 2 Crystallographic Data and Structure Refinement Data for sz multi-component crystals.

	sz+2c4n	**sz+2c5n**	**sz+2hba**	**sz+3hba**	**sz+4hba**
Empirical formula	$C_{19}H_{18}ClN_5O_6S$	$C_{19}H_{18}ClN_5O_6S$	$C_{19}H_{20}N_4O_5S$	$C_{19}H_{20}N_4O_5S$	$C_{19}H_{20}N_4O_5S$
Formula weight/ g·mol^{-1}	479.89	479.89	416.45	416.45	416.45
Temperature / K	173(2)	173(2)	173(2)	173(2)	173(2)
Wavelength / Å	0.71073	0.71073	0.71073	0.71073	0.71073
Crystal system	Orthorhombic	monoclinic	orthorhombic	orthorhombic	triclinic
Space group	*Pbc*2$_1$	*P*2$_1$	*Pbca*	*Pbca*	*P*-1
a / Å	19.2999(6)	6.96450(10)	10.1289(3)	9.9985(3)	7.9638(9)
b / Å	7.7198(2)	19.3894(3)	15.7422(4)	15.7375(4)	9.3601(10)
c/ Å	13.9038(4) Å	15.7238(2)	25.0535(7)	24.6844(7)	13.2882(14)
α /°	90	90	90	90	74.123(4)
β /°	90	90.7000(10)	90	90	75.616(4)
γ /°	90	90	90	90	85.727(4)
V / Å^3	2071.55(10)	2123.14(5)	3994.81(19)	3884.12(19)	922.85(18)
Z	4	4	8	8	2
Density (calculated)/ Mgm^{-3}	1.539	1.501	1.385	1.424	1.499
μ/ mm^{-1}	0.335	0.326	0.201	0.207	0.218
F(000)	992	992	1744	1744	436
Crystal size / mm^3	0.214 x 0.248 x 0.317	0.349 x 0.189 x 0.130	0.441 x 0.284 x 0.238	0.315 x 0.257 x 0.129	0.163 x 0.146 x 0.052
Theta range for data/° collection	2.110 to 28.238.	1.295 to 28.215.	3.057 to 28.334.	2.924 to 28.360.	3.126 to 28.334.
Reflections collected	24549	58621	58505	47634	36343
Independent reflections	5046 [*R*(int) = 0.0545]	10439 [*R*(int) = 0.0482]	4953 [*R*(int) = 0.0405]	4831 [*R*(int) = 0.0748]	4592 [*R*(int) = 0.0511]
Goodness-of-fit on F^2	1.030	1.059	1.021	1.072	1.046
Final R indices [I>2sigma(I)]	R_1 = 0.0366 wR_2 = 0.0707	R_1 = 0.0392 wR_2 = 0.0854	R_1 = 0.0373 wR_2 = 0.0926	R_1 = 0.0452 wR_2 = 0.1134	R_1 = 0.0416 wR_2 = 0.0977
R indices (all data)	R_1 = 0.0560 wR_2 = 0.0785	R_1 = 0.0595 wR_2 = 0.0935	*R*1 = 0.0484 wR_2 = 0.0999	R_1 = 0.0693 wR_2 = 0.1250	R_1 = 0.0555 wR_2 = 0.1039
CCDC Number	1952592	1952593	1952594	1952595	1952596
	sz+4brba	**sz+ba**	**sz+ca**	**sz+ta**	
Empirical formula	$C_{19}H_{19}BrN_4O_4S$	$C_{19}H_{20}N_4O_4S$	$C_{21}H_{22}N_4O_4S$	$C_{20}H_{22}N_4O_4S$	
Formula weight/ g·mol^{-1}	479.35	400.45	426.48	414.47	
Temperature / K	173(2) K	173(2) K	173(2) K	173(2)	
Wavelength / Å	0.71073	0.71073	0.71073	0.71073	
Crystal system	Monoclinic	orthorhombic	monoclinic	monoclinic	
Space group	*P*2$_1$/*n*	*Pbca*	*P*2$_1$/*n*	*P*2$_1$	
a / Å	8.5979(7)	15.1817(3)	a = 8.3614(2)	a = 7.3454(6)	
b / Å	11.8215(10)	14.0288(3)	14.6091(4)	13.3001(11)	
c / Å	19.5587(16)	17.9844(4)	16.9318(5)	11.2172(10)	
α /°	90	90	90	90	
β /°	102.009(3)	90	98.2910(10)	107.585(3)	
γ /°	90	90	90	90	
V / Å^3	1944.4(3)	3830.34(14)	2046.65(10)	1044.65(15)	
Z	4	8	4	2	
Density (calculated) / Mg m^{-3}	1.637	1.389	1.384	1.318	
μ / mm^{-1}	2.257	0.203	0.195	0.188	
F(000)	976	1680	896	436	
Crystal size / mm^3	0.365 x 0.086 x 0.066	0.347 x 0.248 x 0.160	0.514 x 0.317 x 0.254	0.325 x 0.258 x 0.136	
Theta range for data collection	2.983 to 28.356°.	2.265 to 30.749°.	2.899 to 28.315°.	2.909 to 28.356°.	
Reflections collected	26446	46609	40194	19104	
Independent reflections	4840 [*R*(int) = 0.0864]	5970 [*R*(int) = 0.0892]	5084 [*R*(int) = 0.0413]	5182 [*R*(int) = 0.0224]	

Goodness-of-fit on F^2	1.050	1.011	1.081	1.064	
Final *R* indices [I>2sigma(I)]	$R_1 = 0.0485$ $wR_2 = 0.0748$	$R_1 = 0.0465$ $wR_2 = 0.1101$	$R_1 = 0.0372$ $wR_2 = 0.0955$	$R_1 = 0.0336$ $wR_2 = 0.0932$	
R indices (all data)	$R_1 = 0.0889$ $wR_2 = 0.0840$	$R_1 = 0.0917$ $wR_2 = 0.1314$	$R_1 = 0.0478$ $wR_2 = 0.1011$	$R_1 = 0.0375$ $wR_2 = 0.1025$	
CCDC Number	1952597	1952598	1952599	1952600	

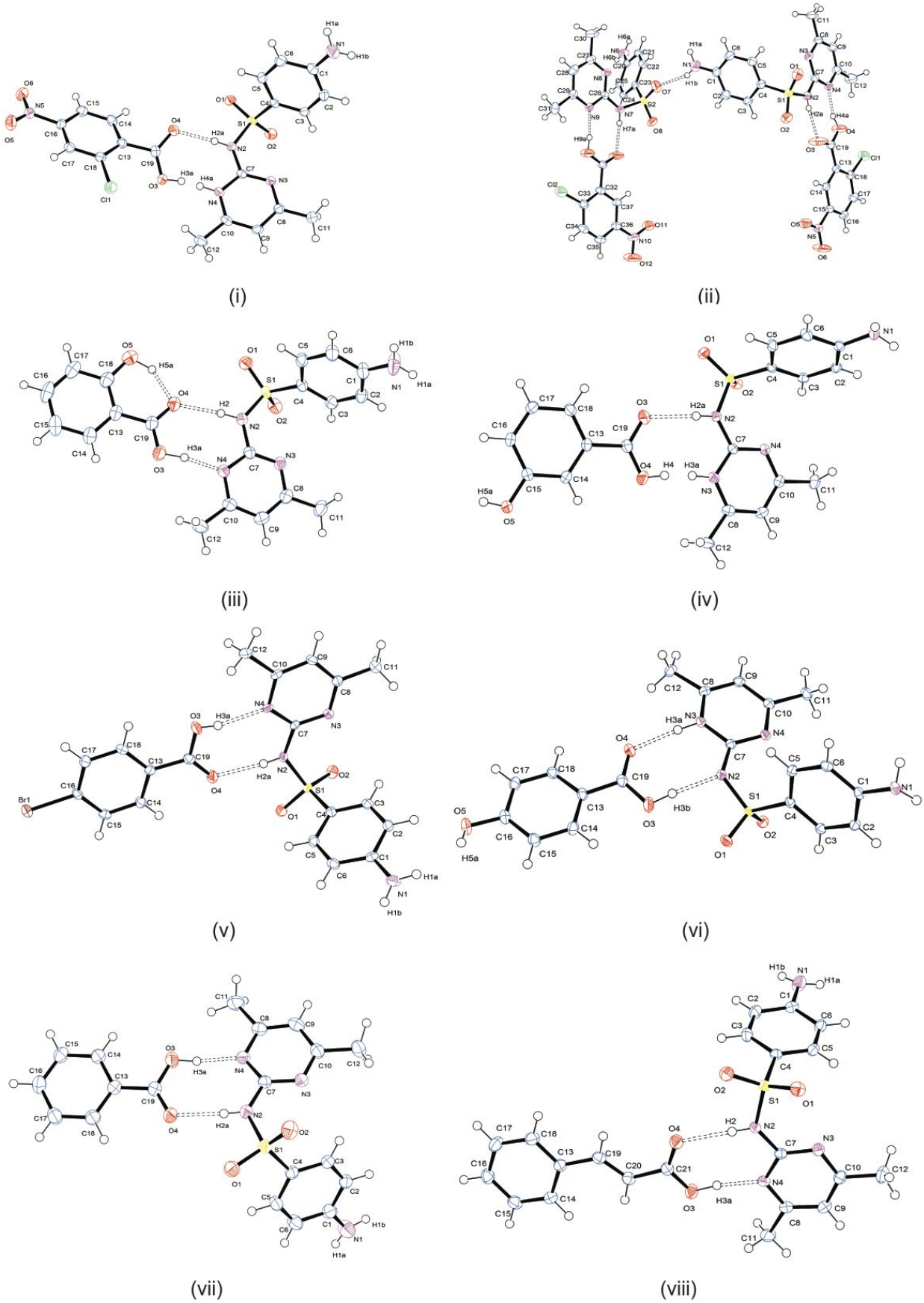

Figure 1 Ortep diagram for (i) **sz+2c4n**, (ii) **sz+2c5n**, (iii) **sz+2hba**, (iv) **sz+3hba**, (v) **sz+4brba**, (vi) **sz+4hba**, (vii) **sz+ba** and (viii) **sz+ca**

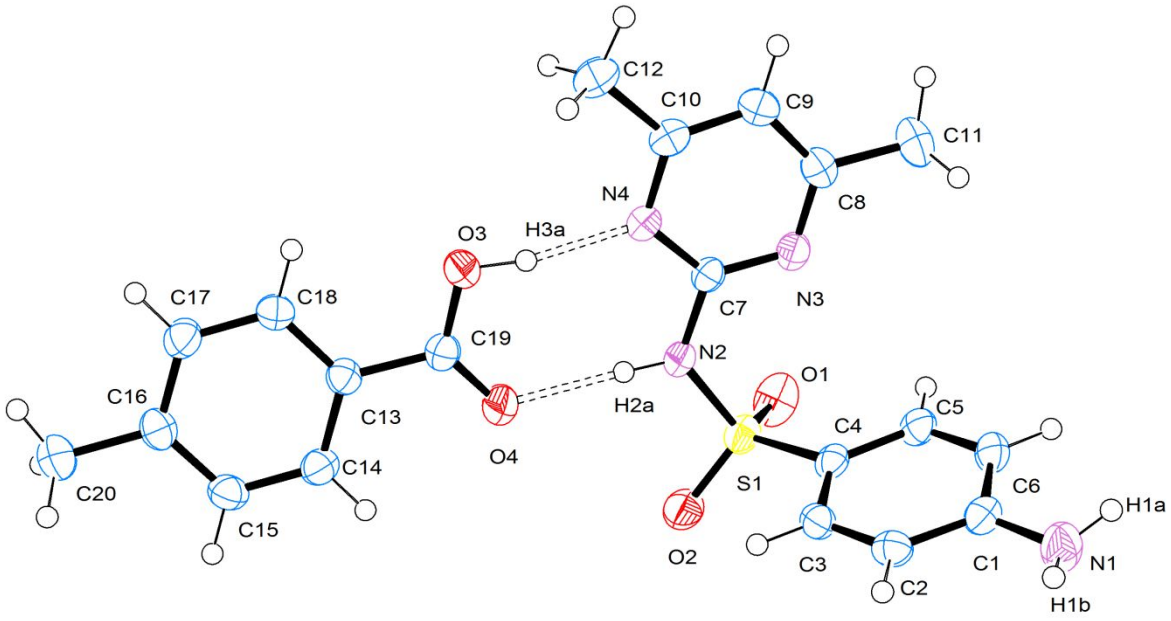

Figure 2 Ortep diagram for **sz+ta**

Table 3 Hydrogen bond table for the multi-component crystals represented in this work.

D-H···A	d(D-H)	d(H···A)	d(D···A)	<(DHA)
		sz+2c4n		
N1-H1A···O4[a]	0.89(5)	2.40(5)	3.083(4)	134(4)
N1-H1B···O5[b]	0.78(5)	2.30(5)	3.032(5)	156(5)
N2-H2A···O4	0.83(5)	1.91(5)	2.731(4)	176(5)
N4-H4A···O3	0.88	1.68	2.560(4)	173
		sz+2c5n		
N1-H1A···O8[c]	0.90(4)	2.20(4)	3.067(5)	159(4)
N1-H1B···O7	0.80(5)	2.15(5)	2.899(4)	156(4)
N2-H2A···O3	0.73(4)	2.06(4)	2.793(4)	172(4)
O4-H4A···N4	0.88(5)	1.80(5)	2.647(4)	159(5)
N6-H6A···O2[d]	0.84(5)	2.36(5)	3.021(4)	136(4)
N6-H6B···O1[e]	0.87(4)	2.14(4)	2.976(4)	162(3)
N7-H7A···O10	0.85(5)	1.92(5)	2.762(4)	173(4)
O9-H9A···N9	0.90(6)	1.74(6)	2.631(4)	172(6)
		sz+3hba		
N2-H2A···O3	0.88	1.93	2.751(2)	155
N1-H1A···O1[f]	0.88(2)	2.24(2)	3.124(2)	177(2)
N1-H1A···S1[f]	0.88(2)	2.95(2)	3.7743(18)	155(18)
N1-H1B···O2[g]	0.88(2)	2.26(2)	3.039(2)	148(2)
O4-H4···N3	0.84	1.89	2.722(2)	171
O5-H5A···N1[h]	0.89(3)	2.01(3)	2.878(2)	165(3)
N3-H3A···O4	0.88	1.86	2.722(2)	166
		sz+4brba		
N1-H1A···O1[c]	0.85(4)	2.27(4)	3.103(4)	169(3)
N1-H1B···O2[i]	0.82(3)	2.36(3)	3.166(4)	168(3)
N2-H2A···O3	0.80(3)	3.12(3)	3.706(4)	132(3)
O3-H3A···N4	0.78(4)	1.93(4)	2.693(3)	168(4)
		sz+4hba		
N1-H1A···O2[c]	0.85(2)	2.23(3)	3.0697(19)	168(2)
N1-H1A···S1[c]	0.85(2)	2.95(3)	3.7585(16)	158(19)
N1-H1B···N4[j]	0.88(2)	2.56(2)	3.430(2)	168(19)
N1-H1B···O2[j]	0.88(2)	2.63(2)	3.1212(18)	116(17)
N3-H3A···O3	0.91(2)	3.06(2)	3.7433(19)	133(17)
O3-H3B···N2	0.93(3)	1.86(3)	2.7765(19)	173(3)
O3-H3B···S1	0.93(3)	2.76(3)	3.5270(14)	141(2)
O5-H5A···N1[k]	0.85(3)	1.97(3)	2.800(2)	165(2)
		sz+ba		
N1-H1A···O3[g]	0.83(3)	2.40(3)	3.084(3)	140(2)
N1-H1B···O2[l]	0.92(3)	2.04(3)	2.955(3)	172(2)
N2-H2A···O3	0.80(3)	2.00(3)	2.792(2)	174(3)
O4-H4···N4	0.94(3)	1.70(3)	2.640(2)	174(2)
		sz+ca		
N2-H2···O3	0.84(2)	3.04(2)	3.6632(15)	134(16)
O3-H3A···N4	0.97(2)	1.71(2)	2.6757(15)	171(2)
N1-H1A···O2[c]	0.85(2)	2.27(2)	3.0828(18)	159(18)
N1-H1B···O1[i]	0.83(2)	2.27(2)	3.0859(18)	168(2)
		sz+2hba		
N2-H2···O4	0.88(2)	1.90(2)	2.7789(16)	175(18)
N1-H1A···O2[a]	0.85(2)	2.14(2)	2.9478(19)	160(2)
N1-H1B···S1[b]	0.91(2)	2.99(2)	3.8674(18)	164(17)
N1-H1B···O1[b]	0.91(2)	2.16(2)	3.057(2)	168(19)
O3-H3A···N4	0.99(3)	1.64(3)	2.6283(15)	171(3)
O5-H5A···O3	0.99(3)	3.56(3)	4.1468(17)	120(19)
		sz+ta		
N1-H1A···O1[o]	0.87(3)	2.08(3)	2.896(3)	155(3)
N1-H1B···O2[n]	0.83(3)	2.19(3)	2.961(3)	154(3)
N2-H2A···O4	0.86(3)	1.90(3)	2.759(2)	177(3)
O3-H3A···N4	0.94(4)	1.81(4)	2.732(2)	168(4)

Symmetry transformations used to generate equivalent atoms:

(a) –x + 1, -y + 2, z - 1/2; (b) x - 1/2, -y + 2, z – 1; (c) x + 1, y, z; (d) x, y, z + 1; (e) x - 1, y, z + 1;
(f) –x + 1/2, y + 1/2, z; (g) –x + 1, y + 1/2, -z + ½; (h) –x + 1/2, -y + 1, z + ½; (i) –x + 3/2, y - 1/2, -z + ½;

(j) –x + 2, -y + 1, -z; (k) –x + 1, -y, -z + 1; (l) –x + 3/2, y + 1/2, z; (m) –x + 1, y - 1/2, -z + 3/2;
(n) –x + 1, y - 1/2, -z + 2; (o) -x, y - 1/2, -z + 2.

Table 4 Comparison of the bond lengths of the carboxyl group of the co-former.

Compound	C19-O3 / Å	C19-O4 / Å	Ratio (long over short)	Long C-O bond of respective co-former in native crystal structure/ Å	Short C-O bond of respective co-former in native crystal structure/ Å
sz+2c4n (salt/cc)	1.266(4)	1.237(4)	1.023	1.247 (**Form I**) 1.288 / 1309 / 1.301 / 1.313 (**Form II**) 13 ***	1.233 (**Form I**) 1.221 / 1.216 / 1.214 / 1.222 (**Form II**) [13]
sz+2c5n* (cc)	1.202(4) / 1.197(4)	1.285(4) / 1.279(4)	1.069 / 1.068	1.295 [14]	1.220 [14]
sz+3hba (salt/cc)	1.250(2)	1.284(2)	1.027	1.317 [15]	1.208 [15]
sz+4brba (cc)	1.311(4)	1.227(4)	1.069	1.309 [16]	1.223 [16]
sz+4hba (cc)	1.318(2)	1.227(2)	1.074	1.278 [17]	1.267 [17]
sz+ba (cc)	1.306(2)	1.228(2)	1.064	1.275 [18]	1.264 [18]
sz+ca ** **(cc)**	1.3127(17)	1.2299(16)	1.067	1.292 [19]	1.254 [19]
sz+2hba (cc)	1.2921(19)	1.2476(18)	1.036	1.311 [20]	1.245 [20]
sz+ta (cc)	1.311(3)	1.224(3)	1.053	1.302 [21]	1.248 [21]

*For the case of **sz+2c5n** the second molecule of 2c5n is also included, as C38-O10 and C38-O9 respectively, separated by a slash. ** For the case of **sz+ca** it is the C21-O3 and C21-O4 bond respectively instead. ***2c4n is polymorphic, with **Form I** having one 2c4n molecule in the asymmetric unit while **Form II** has four 2c4n molecules.

Crystal Structures of sz+4brba

The co-crystal of **sz+4brba** crystalizes in the $P2_1/n$ space group with the asymmetric unit consisting of one molecule of each sz and 4brBA. Sz forms in the amidine tautomer, forming the expected amidine-carboxyl synthon. Sz adopts a v-conformation, which forms wave-like columns along the *c*-axis (**Fig. 3 (i)**), with 4brba sitting in between adjacent columns. However, the pyrimidine rings of sz and 4brba forms a layered structure, with layers separated from each other via the aniline ring of sz.

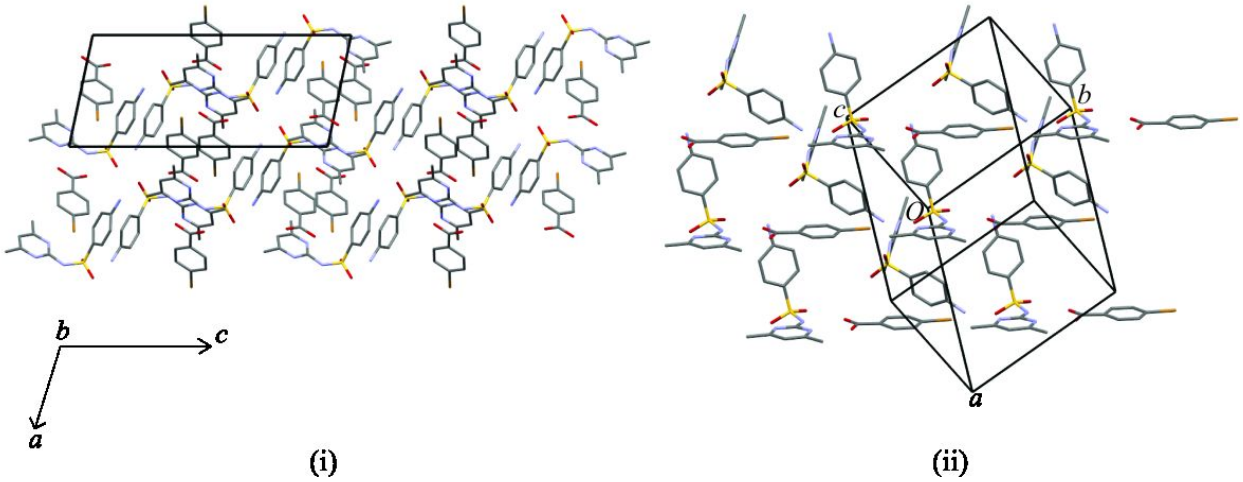

Figure 3 The crystal structure of **sz+4brba** showing (i) the packing viewed down the b-axis, (ii) the layers of the pyrimidine of sz and 4brba separated by the aniline rings.

Crystal Structures of sz+ba, sz+ca and sz+ta

The crystal structure of **sz+ba** has been previously reported 22; while **sz+ca** and **sz+ta** are novel to this work. Co-crystals of **sz+ba**, **sz+ca** and **sz+ta** are described and compared together since the co-formers only consists of one hydrogen bond donor/acceptor – the carboxyl group. From this it should be reasoned that differences in the crystal structures should arise due to the unique aspects of the respective co-former. Co-crystals of **sz+ba**, **sz+ca** and **sz+ta** crystallise in the *Pbca*, $P2_1/n$ and $P2_1$ space groups respectively. In each case the asymmetric unit is made up of one molecule of sz and one molecule of the respective co-former. The co-formers ta, ba and ca contain only one functional group that can form hydrogen bonds – the carboxyl group. In each case, the amidine-carboxyl synthon (Synthon (ii), See **Scheme 2**) formed. **Sz+ca** and **sz+ta** formed the sulfoxide-amino chain synthon (Synthon (iii) see **Scheme 2**), while **sz+ba** did not. Instead, in **sz+ba** the amino group forms a hydrogen bond to one of the oxygen atoms of the sulfoxide group while the other hydrogen bonds to the carboxyl group of **ba** (Synthon (iv) see **Scheme 2)**.

In the packing of the co-crystal of **sz+ba** (**Fig 4 (ii)**), the pyrimidine ring of sz and rings of ba form rows of the aniline ring of sz in the *b*-axis direction separating clusters of **sz+ba** apart. Adjacent dimers of

sz+ba running in the *a*-axis appear T-shaped, with rows interlocking together. In the packing of **sz+ca**, molecules of sz lie in rows down the *b*-axis, alternating between the aniline and pyrimidine rings. This results in the sz molecules forming parallel zig-zag formations, with molecules of ca filling in the gaps between the sz-rows.

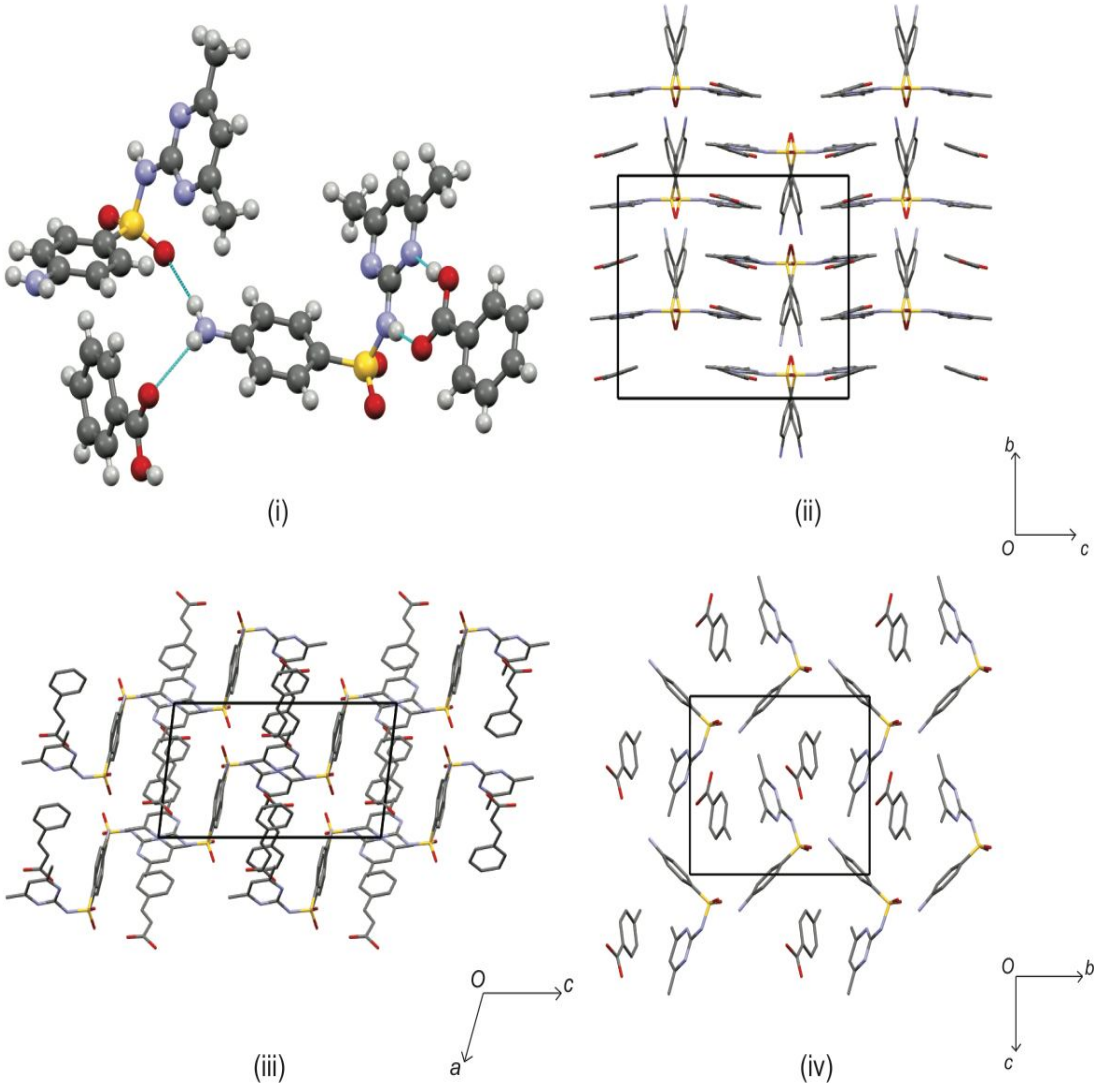

Figure 4 The crystal structure of **sz+ba** showing the hydrogen bonding patterns (i) and its packing (ii). The packing diagrams for **sz+ca** (iii) and **sz+ta** (iv).

Crystal structures of sz + hydroxybenzoic acids

The co-crystals of **sz+2hba** and **sz+3hba** both crystallise in *Pbca* space group, while the co-crystal of **sz+4hba** crystalizes in the *P*-1 space group. In each case, the asymmetric unit is composed of one molecule of sz and each respective conformer. The crystal structures of **sz+4hba** and **sz+2hba** have been previously reported in the literature. [5, 23] Despite using slightly different crystallising conditions (**sz+2hba** used acetone as the solvent, while **sz+4hba** used pure acetonitrile), the same crystal structures were obtained. The co-crystal of **sz+3hba** is novel, hence the synthesis of the former were to prove useful in comparing the changes that may occur due to the shift of the hydroxyl group. In the co-crystal of **sz+3hba**, it was observed that the carboxylic acid proton had only partially transferred to the sz. In the difference Fourier map, there were two clear areas of electron density near O3 and N4. Subsequently, we decided to place a hydroxyl (H3A) and aromatic (H4) hydrogen atom geometrically and give each one a site occupancy of a half. This behaviour is reflected in the ratio of the C-O bonds given in Table 3. For a typical carboxylic acid, the ratio should be greater than 1.5. For a carboxylate, the value should be close to 1.0. In this case, the ratio was found to be 1.027. Hence, we will refer to **sz+3hba** as a mixed salt/co-crystal. **sz+2hba** and **sz+3hba** form the amidine-carboxyl synthon while **sz+4hba** formed the imidine-carboxyl synthon instead. **sz+2hba** and **sz+3hba** form the sulfoxide-amino chains, while **Sz+4hba** do not. Instead only one of the oxygen atoms of the sulfoxide group forms a hydrogen bond with the amino group (N1-H1A···O2). The hydroxyl group for **sz+2hba** forms an intramolecular hydrogen bond as expected. For both **sz+3hba** and **sz+4hba** the hydroxyl group forms a hydrogen bond interaction with the amino group of sz (Synthon (v) see **Scheme 2**).

The packing of the crystal structures of **sz+2hba** and **sz+3hba** are isomorphous, as seen in **Fig 5 (i)** and **(ii)**. Like many of the other crystal structures reported in this work, sz adopts a v-shaped conformation. Both **sz+2hba** and **sz+3hba** form long chains of sz connected by the sulfoxide-amino hydrogen bond, which essentially forms long columns with the hydroxybenzoic acid attached. These columns overall appear in a wave-like structure.

The packing of **sz+4hba** deviates from the previous two. Two molecules of each sz and 4hba form tetramers, which stack together to form a ladder. This ladder is made up of the pyrimidine rings of sz and 4hba making up the steps, while the aniline ring makes up the rail. This description matches the one previously reported. [5]

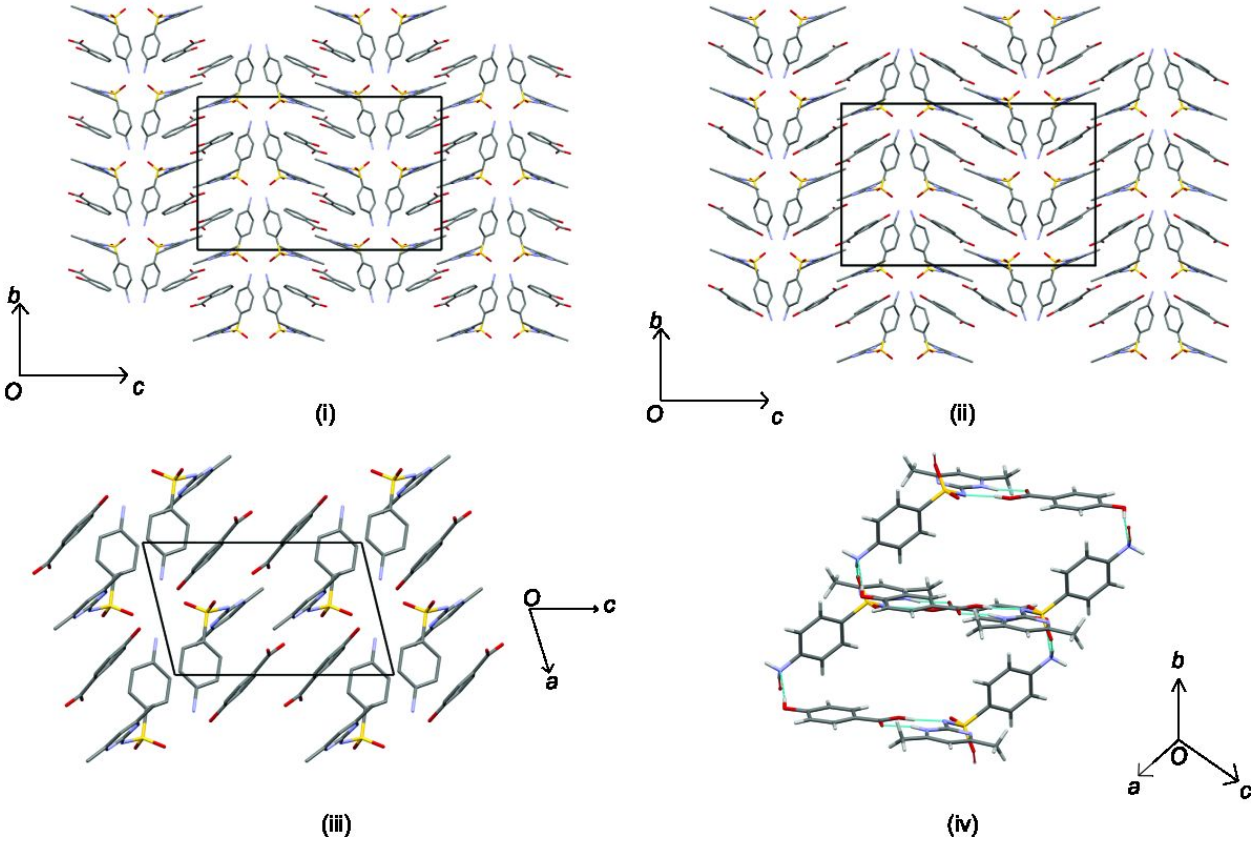

Figure 5 Packing diagram for (i) **sz+2hba** as viewed down the a-axis, (ii) **sz+3hba** as viewed down the *a*-axis and (iii) **sz+4hba** as viewed down the *b*-axis and (iv) two tetramers of **sz+4hba** stacked to show the ladder.

Crystal Structures of sz+2c4n and sz+2c5n

The multi-component crystals of **sz+2c4n** and **sz+2c5n** form a molecular salt and a co-crystal respectively. **Sz+2c4n** and **sz+2c5n** crystalize in the $Pca2_1$ and $P2_1$ space groups respectively. The asymmetric unit for **sz+2c4n** consists of one molecule of each sz and 2c4n, while the one for **sz+2c5n** consists of two molecules of sz and 2c5n. As was the case for **sz+3hba**, **sz+2c4n** was observed to have a

positional disorder of the carboxylic H atom. In the difference Fourier map, there were two clear areas of electron density near O3 and N4. Subsequently, we decided to place a hydroxyl (H4) and aromatic (H3a) hydrogen atom geometrically and give each one a site occupancy of a half. The bond lengths of C19-O3 and C19-O4 for **sz+2c4n** are 1.266(4) and 1.237(4) respectively, giving a ratio of 1.023 and indicating again a mixed salt/co-crystal. Despite being close isomers of each other, 2c4n and 2c5n will exhibit different acid strengths. One approach to determining if a co-crystal or a molecular salt will form is to use the pK_a of the co-formers. If the ΔpK_a ($\Delta pK_a = pK_a$ (Conjugate acid of base) - pK_a (acid)) is greater than 2-3, a molecular salt will form. [24] Anything less than 1 will almost always indicate the formation of a co-crystal. Values between 0-3 are an intermediate case where either a molecular salt or co-crystal could form. For water the pK_a's for sz, 2c4n and 2c5n respectively are 2.07 [25], 1.96 and 2.17, and give ΔpK_a's for **sz+2c4n** and **sz+2c5n** as 0.11 and -0.10 respectively. Although this ΔpK_a could only be truly valid if these crystals were grown from water solution, it still correlates well for the case of **sz+2c5n**.

In addition to being different in being a salt and a co-crystal, some hydrogen bonding patterns are different. The co-crystal of **sz+2c5n** is comparable to many of the other co-crystals presented in this work: the formation of the amidine-carboxyl and the amino-sulfoxide synthons. The nitro group of 2c5n is involved in some weak hydrogen bonding with a neighbouring 2c5n molecule (C16-H16···O12-N10 and C35-H35···O6-N6). In contrast, the sulfoxide group of sz in the salt of **sz+2c4n** does not form the sulfoxide-amino chains that are observed in the other crystal structures. Instead, the amino group of sz forms hydrogen bonds with the carboxylate group and nitro group of 2c4n (N1-H1B···O5 and N1-H1A···O4 respectively). The sulfoxide group forms only weak hydrogen bonds (C11-H11···O1, C14-H14···O2, and C6-H6···O2).

The packing of the crystal structures of **sz+2c4n** and **sz+2c5n** is similar. In both cases sz adopts a v-shaped conformation that has been observed in the other crystal structures. The packing of sz molecules forms channels formed by four sz molecules, which the molecules of 2c4n and 2c5n occupy.

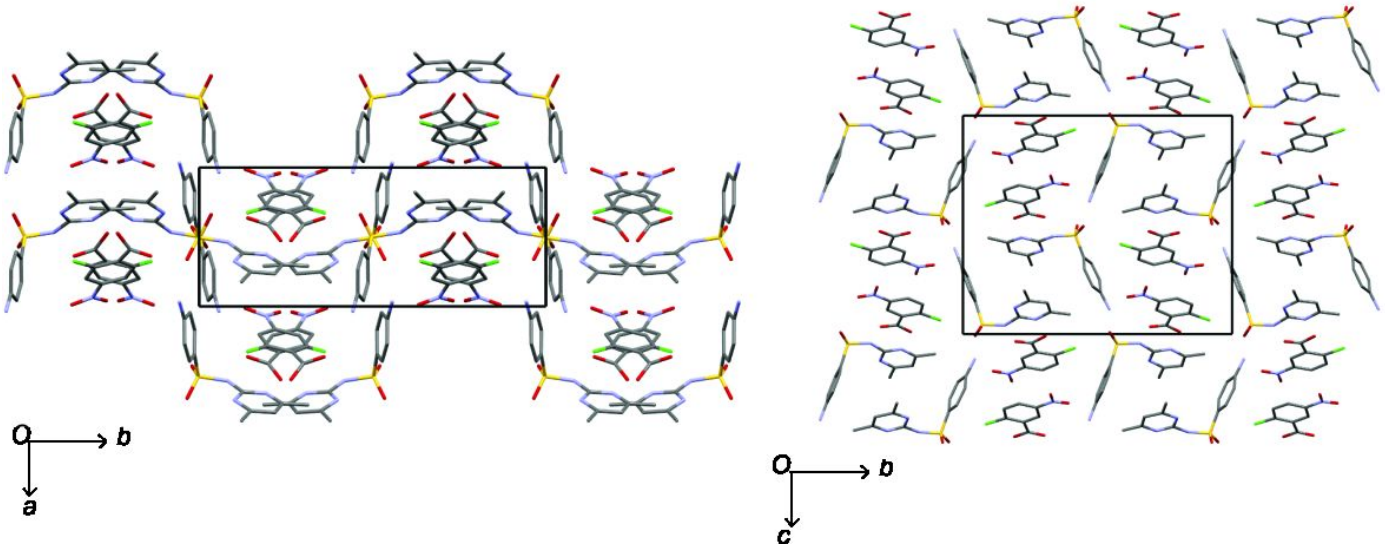

Figure 6 The packing diagrams of the multi-component crystals of **sz+2c4n** as viewed down the *c*-axis (left) and **sz+2c5n** with the *a*-axis coming out of the plane (right).

Infrared Spectroscopy

Infrared spectroscopy can be used to determine the formation of molecular salts or co-crystals by comparing the spectrum of the multi-component crystal with the spectra of the parent co-formers. A shift of a peak between the spectrum of the parent co-former and the spectrum of the multi-component crystal is typically expected. For this work, FT-IR spectra were obtained and are presented in Fig. 7.The stretching frequencies of the primary amino group of **sz** ($-NH_2$) and the sulfonamide group (-NH) are then compared to that of the parent co-former. **Table 7** contains the wavenumbers associated with the *sym* and *asym* stretching frequencies of the primary amino group and the stretching frequency of the sulfonamide group. It is clear that for most of the multi-component crystals, there is a shift in the expected stretching frequencies.

In particular it should be noted that for the spectrum of **sz+2c4n** a broad band is observed over the 1500-1650 cm^{-1} region, which is not observed for the other multi-component crystals presented in this work. This broad band is typically associated with a carboxylate, which infers that the multi-component crystal of **sz+2c4n** is indeed a molecular salt, in contrast to the refinement model we used in the crystal structure.

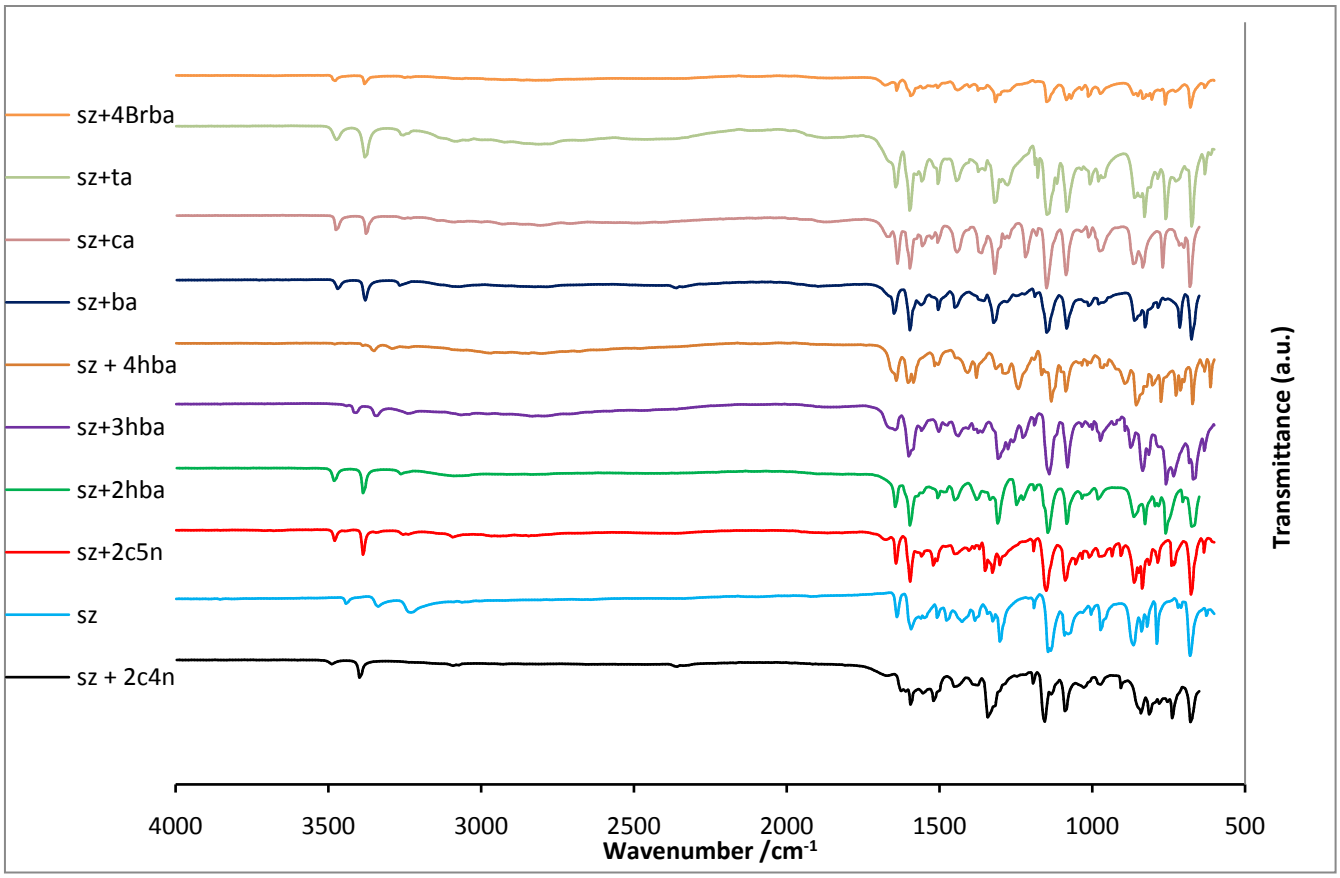

Figure 7 The FTIR spectra obtained for the **sz** and the multi-component crystals of **sz**.

Table 5 Peak shift assignments for the IR spectra of **sz** and the multi-component crystals of **sz.** Note, values in brackets indicate the shift of the peak compared to pure **sz**.

Peak Assignment	Wavenumber /cm^{-1}
sz	
Amine ν(NH_2) *sym*	3346
Amine ν(NH_2) *asym*	3445
Sulfonamide (NH)	3238
sz+2c4n	
Amine ν(NH_2) *sym*	3396 (+50)
Amine ν(NH_2) *asym*	3488 (+43)
Sulfonamide (NH)	3094 (-144)
sz+2c5n	
Amine ν(NH_2) *sym*	3388 (+42)
Amine ν(NH_2) *asym*	3483 (+38)
Sulfonamide (NH)	3247 (+9)
sz+2hba	
Amine ν(NH_2) *sym*	3380 (+34)
Amine ν(NH_2) *asym*	3485 (+40)
Sulfonamide (NH)	3251 (+13)
sz+3hba	
Amine ν(NH_2) *sym*	3352 (+6)
Amine ν(NH_2) *asym*	3419 (-26)
Sulfonamide (NH)	3230 (-8)
sz+4hba	
Amine ν(NH_2) *sym*	3359 (+13)
Amine ν(NH_2) *asym*	3376 (-69)
Sulfonamide (NH)	3283 (+45)
sz+4Brba	
Amine ν(NH_2) *sym*	3384 (+38)
Amine ν(NH_2) *asym*	3486 (+41)
Sulfonamide (NH)	3241 (+3)
sz+ba	
Amine ν(NH_2) *sym*	3373 (+27)
Amine ν(NH_2) *asym*	3460 (+15)
Sulfonamide (NH)	3271 (+33)
sz+ca	
Amine ν(NH_2) *sym*	3371 (+25)
Amine ν(NH_2) *asym*	3477 (+32)
Sulfonamide (NH)	3265 (+29)
sz+ta	
Amine ν(NH_2) *sym*	3381 (+35)
Amine ν(NH_2) *asym*	3480 (+32)
Sulfonamide (NH)	3247 (+9)

Differential Scanning Calorimetry Results

The multicomponent crystals were analysed by DSC. Samples were heated at a rate of 10 °C/min from 25 °C to 250 °C, which were then cooled back to 25 °C at a rate of 10 °C/min. In each case, upon cooling, no further thermal events were observed. With the exception of **sz+4brba** and **sz+ca**, the DSC curve for each sample showed only one single endothermic peak, which corresponds to melting. These curves are plotted in Fig. 8, with thermodynamic data in Table 2. The DSC curves for **sz+4brba** and **sz+ca** were plotted separately and are in Fig. 9. **sz+4brba** show two endothermic peaks: one broad peak occurring at 125 °C and one peak at 204 °C. **sz+ca** show two peaks occurring at 188 °C and 209 °C respectively.

In order to determine what the additional peaks observed in the crystals of **sz+4Brba** and **sz+ca** are, crystals were mounted on a glass fibre and heated *in situ* in the diffractometer. These crystals were heated from 25 °C up to the temperature at which the first thermal event were observed. The unit cell parameters were collected at every 10 °C interval to monitor if any significant change occurs. In both cases, as soon as the crystal reached the temperature at which the first thermal event occurs, no diffraction spots were observed in the diffraction image. These crystals were observed to have changed from being transparent to being opaque. This implies that the phase change associated with the first thermal event of the DSC curves for both cases is a phase change from being crystalline to being amorphous.

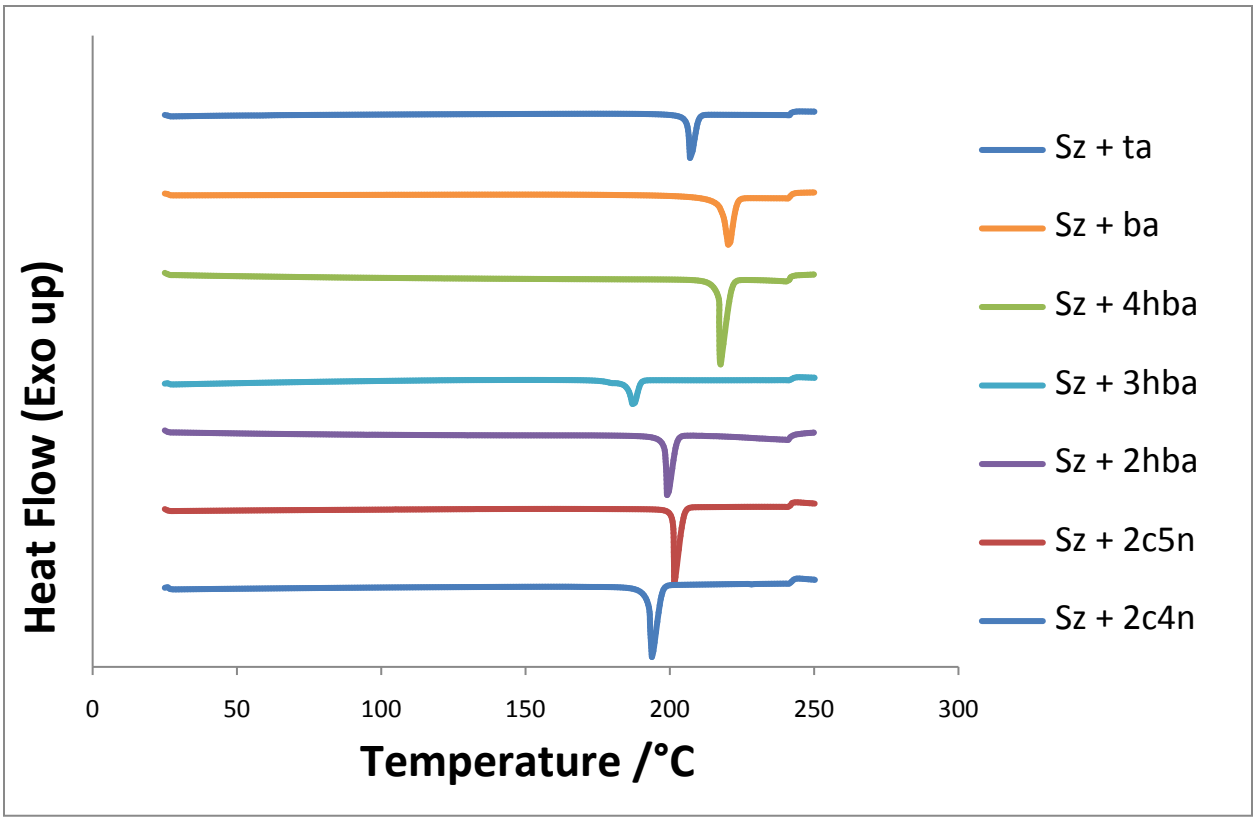

Figure 8 DSC curves for co-crystals which only show melting.

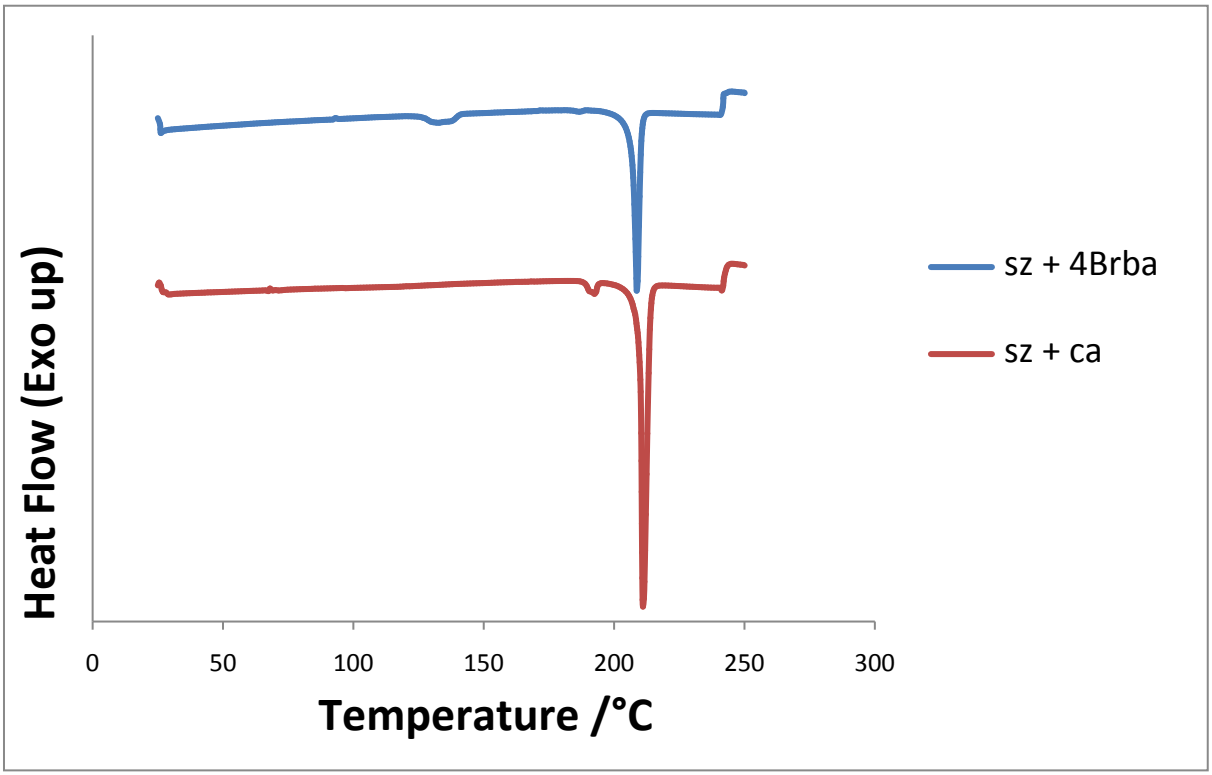

Figure 9 DSC curves for **sz+4brba** and **sz+ca** showing the additional endothermic peaks.

Table 6 Thermodynamic data for the endothermic peaks of the multi-component crystals.

Co-crystal/salt	Onset / °C	Peak / °C	Enthalpy / kJ mol^{-1}
sz+2c4n	192.1	193.8	72.5
sz+2c5n	200.8	201.6	72.6
sz+2hba	198.0	199.2	64.1
sz+3hba	184.8	187.4	75.3
sz+4hba	214.2	217.6	57.5
Sz+4Brba (crystalline →amorphous phase transition)	126.1	132.8	10.5
sz+4Brba (Melting phase transition)	206.6	208.8	58.3
sz+ca (crystalline →amorphous phase transition)	188.7	192.7	2.3
sz+ca (Melting phase transition)	209.8	211.2	51.2
sz+ba	217.4	220.5	66.4
sz+ta	203.9	208.0	54.0

Conclusions

Nine multi-component crystals were synthesised and characterized. Among **sz+ba**, **sz+ca** and **sz+ta**, structural feature varied widely despite having the same set of hydrogen bond synthons. **sz+2hba** and **sz+3hba** were found to be isomorphous and favoured the amidine-carboxyl synthon, while **sz+4hba** differed from the previous two both in terms of packing as well as the imidine-carboxyl synthon. **sz+2c4n** and **sz+2c5n** formed a salt and co-crystal respectively and showed vast differences between the two in terms of packing and synthons despite being isomers of each other. Finally the DSC showed that

the multi-component crystals have different melting points from each other and the co-formers that make it up. Thus, co-formers containing the carboxyl group have great potential for forming a multi-component crystal with sz. Therefore **sz** could prove useful as a potential co-former itself for compounds or even other API's which feature carboxylic acid functional groups.

References

(1) Blagden N., de Matas M., Gavan P.T., York P., *Crystal engineering of active pharmaceutical ingredients to improve solubility and dissolution rates.*, Advanced Drug Delivery Reviews, 2007, **59**, 617 – 630

(2) Pouton C.W., *Formulation of poorly water-soluble drugs for oral administration: Physicochemical and physiological issues and the lipid formulation classification system*, European Journal of Pharmaceutical Sciences, 2006, **29**, 278-287

(3) Schultheiss N., Newman A., *Pharmaceutical Cocrystals and Their Physicochemical Properties* Crystal Growth & Design, 2009, **9**, 2950–2967

(4) Vishweshwar P., Mcmahon J., Bis J.A., Zaworokto M.J., *Pharmaceutical co-crystals.*, J. Pharm Sci, 2006, **95**, 499-516

(5) Ghosh S., Bag P.P., Reddy C.M., *Co-Crystals of Sulfamethazine with Some Carboxylic Acids and Amides: Co-Former Assisted Tautomerism in an Active Pharmaceutical Ingredient and Hydrogen Bond Competition Study*, Cryst. Growth Des., 2011, **11**, 3489 – 3503.

(6) Lu J., Cruz-Cabeza A.J., Rohani S., Jennings M.C., *A 2:1 sulfamethazine–theophylline cocrystal exhibiting two tautomers of sulfamethazine*, Acta Cryst., 2011, **C67**, o306–o309

(7) Kumar V., Thaimattam R., Dutta S., Munshi P., Ramanan A., *Structural landscape of multicomponent solids based on sulfa drugs*, CrystEngComm, 2017, **19** , 2914–2924

(8) Maury L., Rambaud J., B Pauvert., Lasserre Y., Berge G., Audra M., *Physicochemical and structural study of sulfamethazine*, J. of Pharmaceutical Sciences, 1985, **74**

(9) *Bruker, SAINT+, version 6.02 (including XPREP), Bruker AXS Inc.*, Madison, WI, USA, 1999., CrystEngComm, 2012, **14**, 6362–6365

(10) G. M. Sheldrick, *SHELX, release 97-2 (includes SHELXS and SHELXL)*, University of Göttingen, 1997.

(11) L. Farrugia, *ORTEP-3 for Windows - a version of ORTEP-III with a Graphical User Interface (GUI)*, Journal of Applied Crystallography, 1997, **30**, 565.

(12) C. F. Macrae, P. R. Edgington, P. McCabe, E. Pidcock, G. P. Shields, R. Taylor, M. Towler, J. van de Streek, *Mercury: visualization and analysis of crystal structures*, J. Appl. Cryst., 2006, **39**, 453-457

(13) Barsky, I., Bernstein, J., *Stephens, P. W., & Stone, K. H., The study of the polymorphic system of 2-chloro-4-nitrobenzoic acid,* New Journal of Chemistry, 2008, **32**, 1747

(14) Ferguson, G., & Sim, G. A., *336. X-ray studies of molecular overcrowding. Part IV. The cystal and molecular structure of 2-chloro-5-nitrobenzonic acid*, Journal of the Chemical Society (Resumed), 1962, **336**, 1767.

(15) Clevers, S., Simon, F., Sanselme, M., Dupray, V., & Coquerel, G., *Monotropic Transition Mechanism of m-Hydroxybenzoic Acid Investigated by Temperature-Resolved Second Harmonic Generation,* Crystal Growth & Design, 2013, **13**, 3697–3704.

(16) Ohkura, K., Kashino, S., Haisa, *The Crystal and Molecular Structure of p-Bromobenzoic Acid*, M., Bulletin of the Chemical Society of Japan, 1972, **45**, 2651–2652.

(17) Du, J. J., Stanton, S. A., Williams, P. A., Ong, J. A., Groundwater, P. W., Overgaard, J. Platt J., Hibbs, D. E., *Using Electron Density to Predict Synthon Formation in a 4-Hydroxybenzoic Acid: 4,4'-Bipyridine Cocrystal*, Crystal Growth & Design, 2018, 18, 1786–1798.

(18) Bruno, G., Randaccio, L., *A refinement of the benzoic acid structure at room temperature* Acta Crystallographica, 1980, **B36**, 1711–1712.

(19) Wierda, D. A., Feng, T. L., Barron, A. R., *Structure of α-trans-cinnamic acid*, Acta Crystallographica, 1989, **C45**, 338–339.

(20) Munshi, P., & Guru Row, T. N., *Intra- and intermolecular interactions in small bioactive molecules: cooperative features from experimental and theoretical charge-density analysis*, Acta Crystallographica, 2006, **B62**, 612–626.

(21) Hathwar, V. R., Thakur, T. S., Row, T. N. G., & Desiraju, G. R., *Transferability of Multipole Charge Density Parameters for Supramolecular Synthons: A New Tool for Quantitative Crystal Engineering*, Crystal Growth & Design, 2011, **11**, 616–623.

(22) Arman H.D., Kaulgud T., Tiekink E.R.T., *4-Amino-N-(4,6-dimethylpyrimidin-2-yl)-benzenesulfonamide–benzoic acid (1/1),* Acta Cryst. (2010). E66, o2430

(23) Patel U., Haridas M., Singh T.P., *Structure of the 1:1 complex between 4-amino-N-(4,6-dimethyl-2-pyrimidinyl)benzenesulfonamide (sulfadimidine) and 2-hydroxybenzoic acid (salicylic acid)*, Acta Cryst., 1988, **C44**, 1264-1267

(24) Cruz-Cabeza A.J., *Acid–base crystalline complexes and the pK_a rule*, CrystEngComm, 2012, **14**, 6362–6365

(25) Qiang Z., Adams C., *Potentiometric determination of acid dissociation constants (pKa) for human and veterinary antibiotics*, Water Research, 2004, **38**, 2874–2890

For Table of Contents Use Only

Synthesis and characterization of a series of sulfamethazine multi-component crystals with various benzoic acids

Matthew C. Scheepers and Andreas Lemmerer

Nine multi-components crystals consisting of sulfamethazine with benzoic acid and its derivatives were synthesized. Eight of these multi-component crystals were co-crystals while one formed a salt. The amidine/imidine group of sulfamethazine formed hydrogen bonds with the carboxylic acid of the benzoic acid. These crystals were characterized by Single Crystal X-Ray Diffraction, Differential Scanning Calorimetry and Powder X-Ray Diffraction.

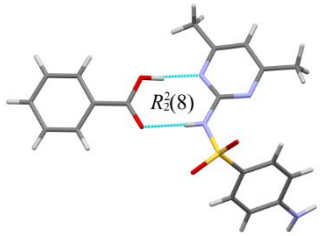

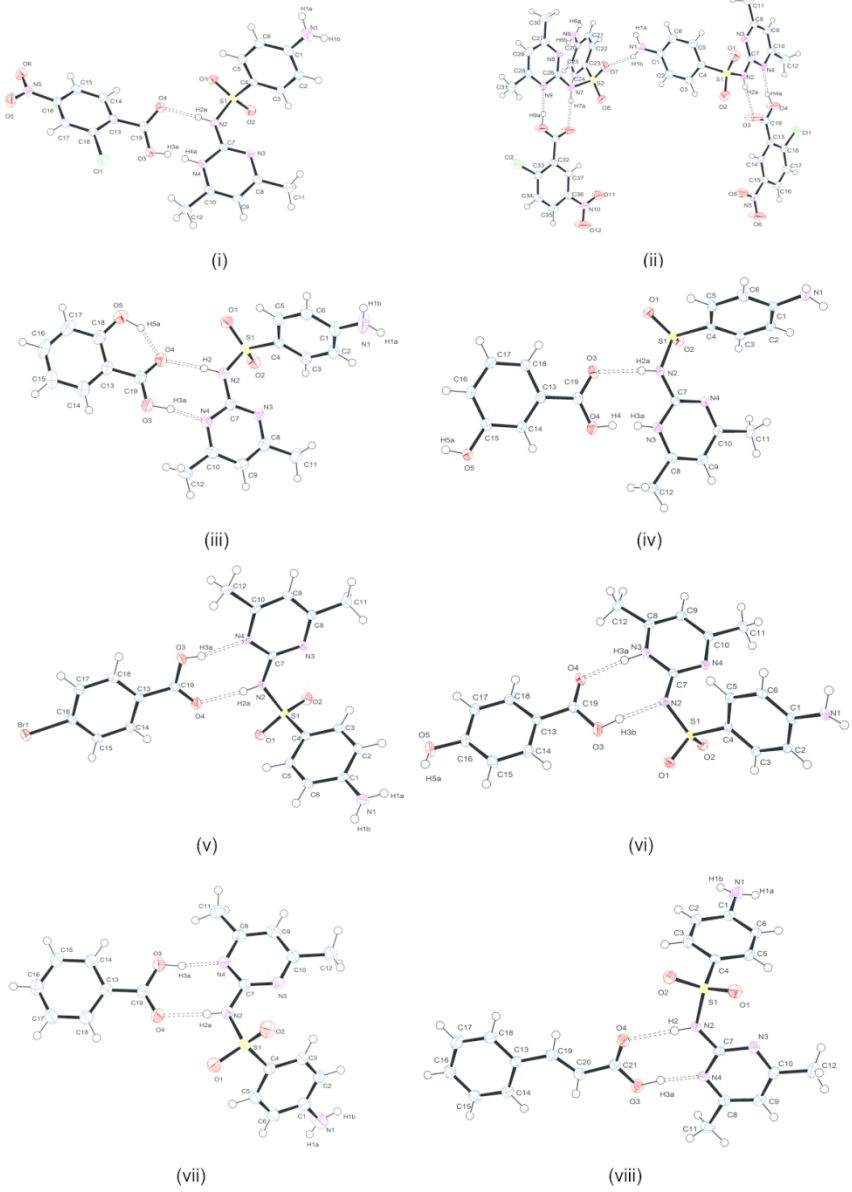
(i)
(ii)
(iii)
(iv)
(v)
(vi)
(vii)
(viii)

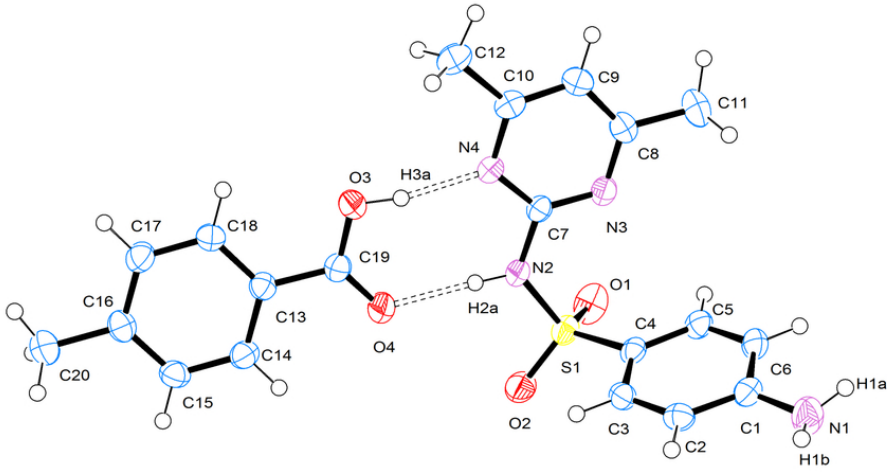

80x60mm (300 x 300 DPI)

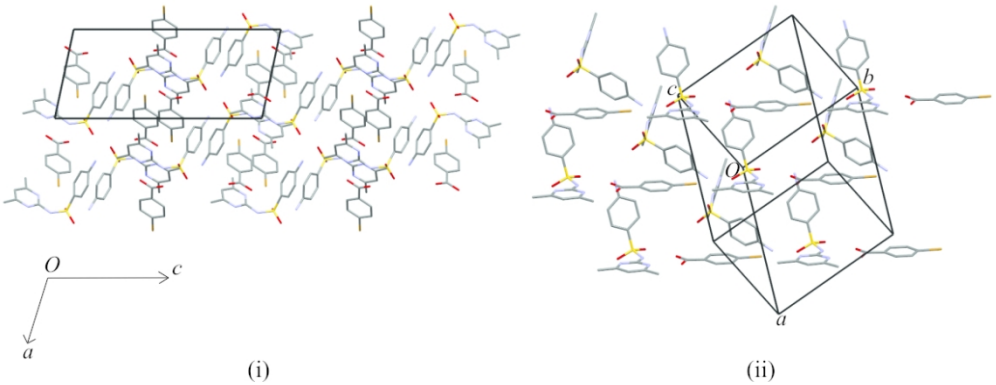

(i) (ii)

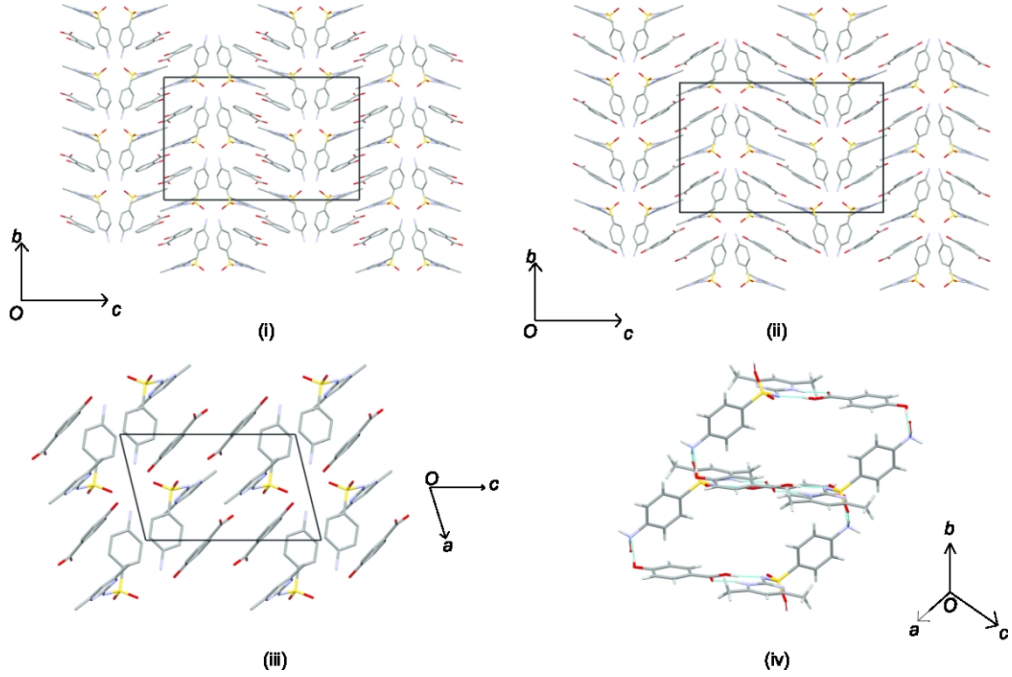
b
O
c
(i)
b
O
c
(ii)
O
c
a
(iii)
b
O
a
c
(iv)

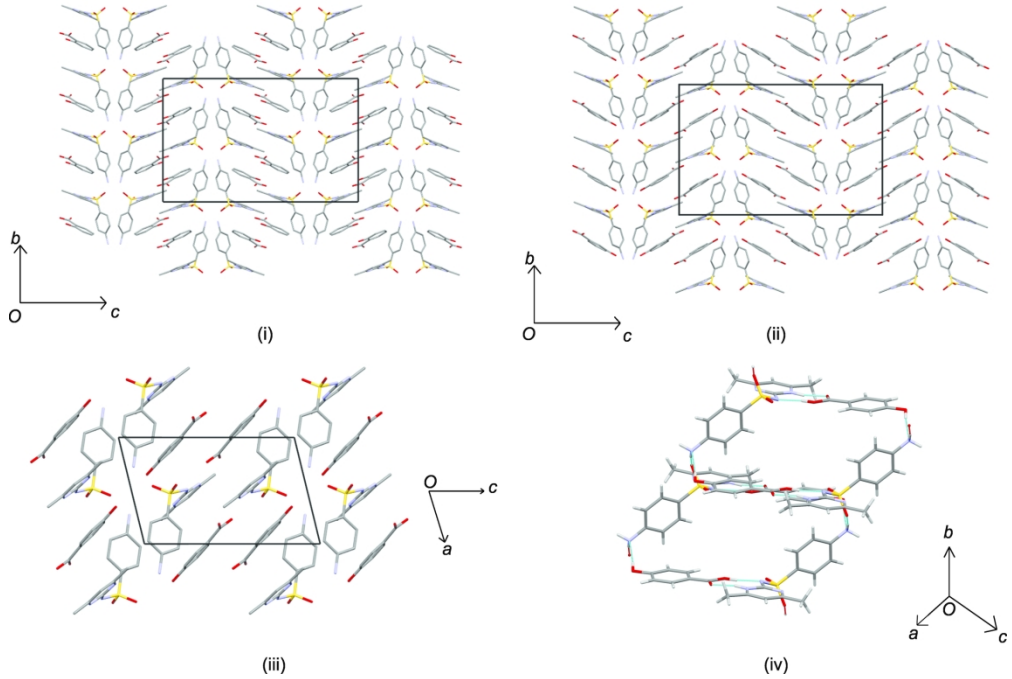

200x138mm (300 x 300 DPI)

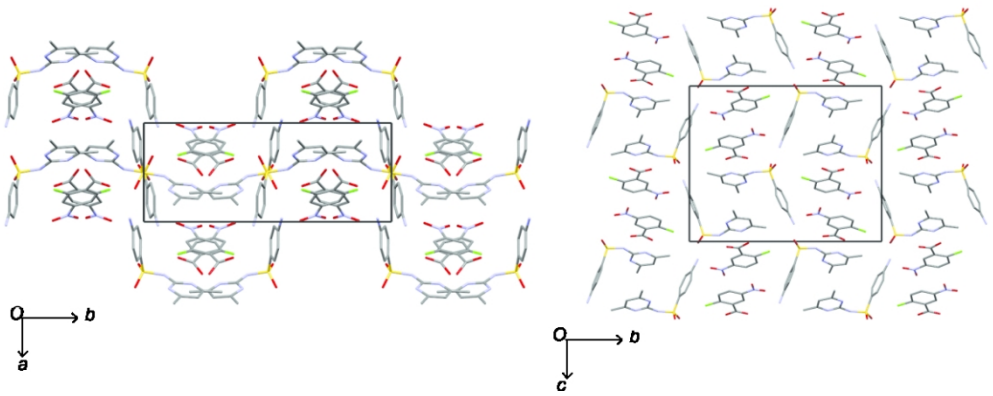
O
b
a
O
b
c

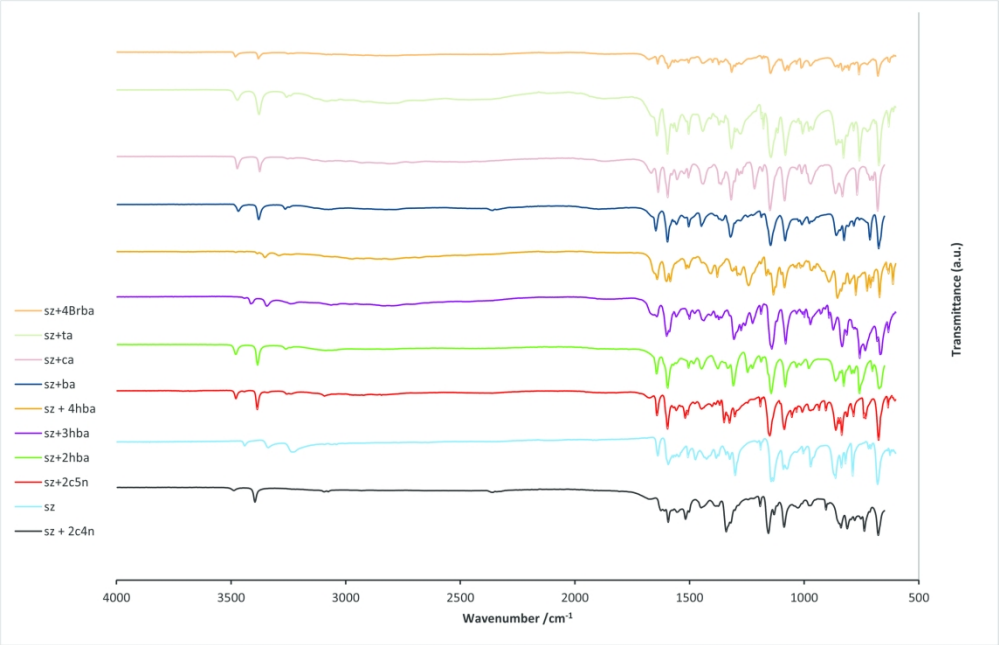

201x130mm (300 x 300 DPI)

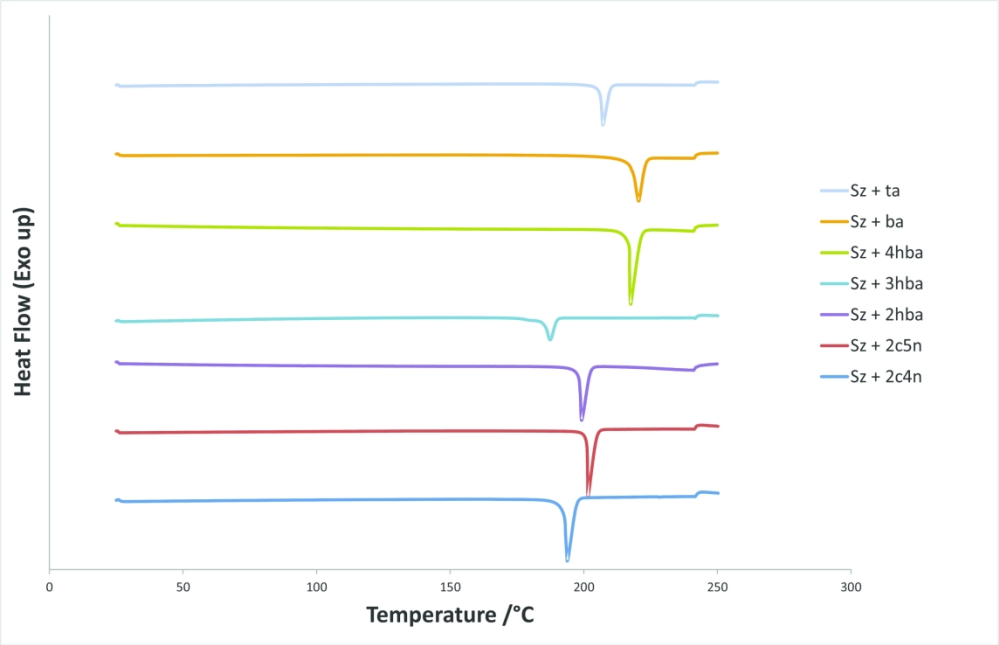

209x135mm (300 x 300 DPI)

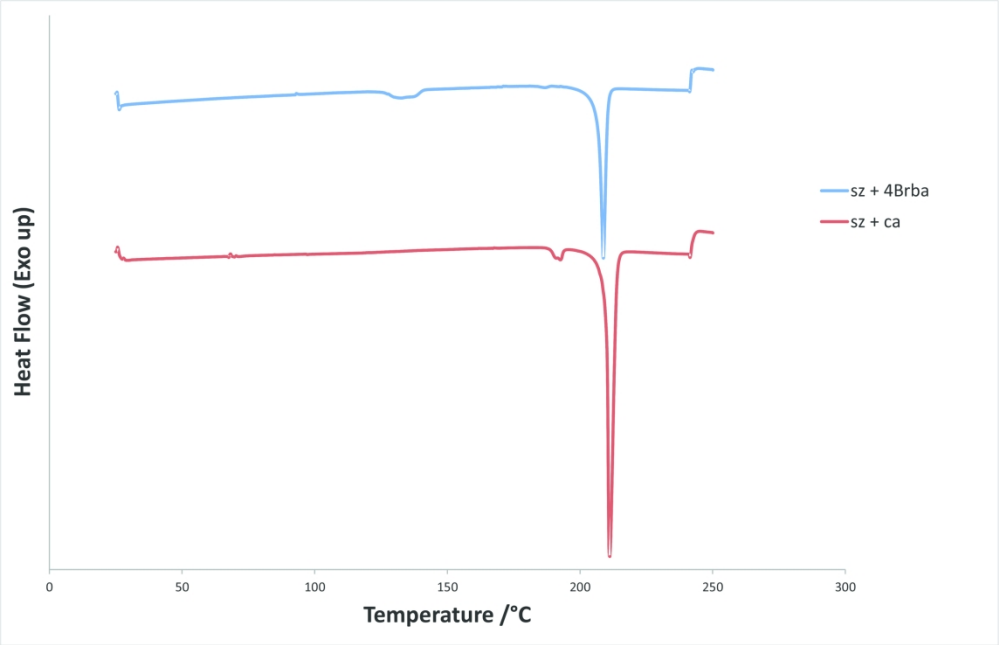

209x135mm (300 x 300 DPI)